The variety of phosphor $Ca_2MgSi_2O_7:Eu^{2+}$ emission color affect white light LEDs

Pham Van De[1], My Hanh Nguyen Thi[2]
[1]Faculty of Engineering, Dong Nai Technology University, Bien Hoa City, Vietnam
[2]Faculty of Mechanical Engineering, Industrial University of Ho Chi Minh City, Ho Chi Minh City, Vietnam

Article Info

Article history:

Received Mar 22, 2024
Revised Nov 28, 2024
Accepted Feb 27, 2025

Keywords:

$Ca_2MgSi_2O_7:Eu^{2+}$
Color deviation
Luminous flux
WLED
YAG:Ce

ABSTRACT

The conventional phosphor-converted white light emitting diode (WLED) suffers from several drawbacks relevant to heat generation and low rendered performance. Thus, using ultraviolet LEDs was introduced as a solution. It is essential to choose the phosphors with high stability that can activated under 350-410 nm to be compatible with the chips. Rare-earth-doped silicate phosphor is among the most reserched materials for solid-state light devices, thanks to its high stability and low-cost production. This work presents the Eu^{2+}-doped $Ca_2MgSi_2O_7$ green phosphor to serve the pursuit of comprehensively enhancing the WLED performances. The f–d transitions and Eu^{2+} ions mixture take possession of two seperate cation spots in main grids with the help of two emission peaks, one at 465 nm and another at 520 nm. The composition of $YAG:Ce^{3+}$ and $Ca_2MgSi_2O_7:Eu^{2+}$ phosphors, and a near-UV chip of 370nm were utilized to compose WLEDs. Results show that by increasing the $Ca_2MgSi_2O_7:Eu^{2+}$ phosphor amount, the lumen output, correlated color homogeneity, and color rendering factors can be improved. The paper emphasizes the necessity for the optimal selection of the $Ca_2MgSi_2O_7:Eu^{2+}$ phosphor concentration, which would be about 10 wt%. The phosphors could be promising in making green-induced white luminous materials for white pc-LEDs with near UV-base.

Corresponding Author:

My Hanh Nguyen Thi
Faculty of Mechanical Engineering, Industrial University of Ho Chi Minh City
Ho Chi Minh City, Vietnam
Email: nguyenthimyhanh@iuh.edu.vn

1. INTRODUCTION

Due to its outstanding qualities like brightness, extended lifespan, optimal applied voltage, and good power efficacy, light-emitting diodes with a phosphor-converted mechanism (pc-LEDs) are now prospective options for solid-state illumination [1]–[3]. For generating white light, merging a LED chip which has one blue or ultraviolet (UV) color using down-transforming phosphor samples for making PC-LEDs. The initial commercial pc-LED was invented by mixing blue LED with a combination containing cerium incorporated with yttrium aluminum garnet (YAG:Ce) capable of emitting yellow light. On the other hand, this method has drawbacks such as heat extinguishing, poor hue performance, and a restricted viewing area.

To overcome the issues persistent in the conventional LED structure, there has been a lot of interest in utilizing UV or near-UV (between 365 and 410 nm) LEDs for producing the phosphor-converted white LEDs. An essential note in fabricating such a LED structure is the selection of phosphor samples with an excitative wavelength within the 350-410nm span for a superior color rendering index. Recently, sulfide phosphors like ZnS:Cu, Al [4] or $SrGa_2S_4:Eu^{2+}$ [5] are the green-emitting phosphors that is most widely employed for white LEDs. However, they have low chemical stability to against moistness as well as show significant degradation during the injection of LED chip. The exceptional properties of rare-earth-ion-doped silicate phosphors make them a compelling choice for a wide range of applications. These phosphors offer outstanding chemical and thermal stability, customizable color emission, long-lasting afterglow effects, and cost-effectiveness. Their potential applications include fluorescent lamps, white LEDs, traffic lights, and display components [6], [7].

It is widely acknowledged that the phosphorescence of Eu^{2+} in most host materials stems from 4f–5d transitions, with the peak positions in the emission spectrum being heavily influenced by the environment of the Eu^{2+} ions in the host lattices [8]. The ground states of the rare-earth Eu^{2+} ion with bivalent characteristic possess the $4f^7$ electron arrangement, while the excited statuses have the $4f^6 5d^1$ electron design. The $4f^7$–$4f^6 5d^1$ transitions are responsible for Eu^{2+} broadband's absorption and luminescence. Under various base latticeworks, Eu^{2+} emission may span the UV to red-spectrum area. However, in most hosts, the luminescence of Eu^{2+} is predominantly observed in the blue and green ranges.

Lots of research has been conducted to investigate the illumination from rare-earth doped $M_2MgSi_2O_7$ alkaline silicate phosphor (M = Sr, Ba, Ca) [9]–[11]. This paper describes the luminescence of Eu^{2+}-doped $Ca_2MgSi_2O_7$. According to the standpoint of crystal field energy and main covalence, the emitting hue change related to the two emitting ranges of Eu^{2+} is also a part of the study. The merger between 370-nm LED chips and phosphor samples was also simulated to make greenish-white pc-LEDs. The simulation results collected using the MATLAB program are then presented and discussed. The concentration variation of the Eu^{2+}-doped $Ca_2MgSi_2O_7$ phosphor is particularly demonstrated in connection to the lumen output, CCT values, and chromatic rendition of the WLED.

2. COMPUTATIONAL SIMULATION

2.1. Preparing $Ca_2MgSi_2O_7$:Eu^{2+}

Initially, the process of sysnthesizing $Ca_2MgSi_2O_7$:Eu^{2+} phosphor is summarized for reference. The obtained phosphor has the green emission with a peak at 2.29 eV and an emitting breadth (FWHM) of 0.37 eV. The phosphor can be stimulated by UV sources with the effectiveness of ++ (4.88 eV), ++ (3.40 eV); approximately 25%. To achieve the required tetragonal (ackermanite) phosphor, please follow the composition as Table 1. In the beginning, all raw ingredients are blended in methanol combined with a few cubic centimeters of water. After a while, the mixture is let to dry in air, and then ground or milled into powder. Subsequently, the powder is burned in capped quartz tubes, with N_2 under 1,000 ºC in 1 hour, followed by a re-grinding step. After that, the obtain powder was re-burned for an hour in capped quartz tubes filled with CO. The burning temperature for this time was 1,150 ºC [12]–[15].

Table 1. Consituents for $Ca_2MgSi_2O_7$:Eu^{2+}

Ingredient	Mole %	By weight (g)
CaO	114	64
MgO	100	40
SiO_2	210	126
Eu_2O_3	2 (of Eu)	3.5
$MnCO_3$	4	4.6
NH_4Cl	40	21.4

2.2. WLED simulation

The phosphor coating of genuine WLEDs would be recreated through plain silicone layers by employing the LightTools 9.0 program along with MATLAB program and Monte Carlo method [16], [17]. Two separate stages make up this modeling:

- Establishing and developing WLED lamp setup models and optic properties.
- The $Ca_2MgSi_2O_7$:Eu^{2+} dosage range then effectively regulates the impacts associated to the optic of phosphor compounding.

To ascertain the impact of $Ca_2MgSi_2O_7$:Eu^{2+} phosphors on the performance in LED apparatuses, the simulation is carried out under three median CCT levels of 6000 K, 7000 K, and 8000 K. Figure 1 shows WLED lights with conventional phosphor compounding as well as one mean CCT reaching 8000 K in particular. In addition, the LED setting primarily includes a reflector, LED chips, and the phosphor layer. The reflector has the underneath length of ~8 mm, height of ~2.07 mm, and the upper covering lengthiness of ~9.85 mm. The conformal combination would be put in applications to nine chips with a 0.08 mm thickness. Each LED chip would be linked to the reflector's gap by a square base zone of 1.14 mm^2 and an altitude of 0.15 mm.

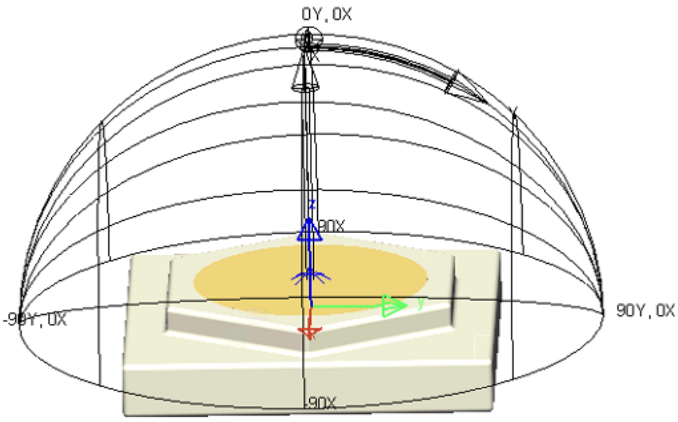

Figure 1. Picture depicting a WLED device

3. RESULTS AND ANALYSIS

3.1. Photoluminescence characteristic of the phosphor

The PL spectra of $Ca_2MgSi_2O_7:Eu^{2+}$ phosphors can be greatly affected by the Eu^{2+} concentration (x) [11]. It is said by Blasse [18]–[20] that one activator for each of the V/x_cN when the trigger would be set primarily under Z granule locations. x_c indicates the essential dosage, the quantity for Z ions within one-unit cellule is N. V represents a cellule's capacity. One standard trigger granule will be for one V/x_cN. The critical transference span (R_c) of a sphere with this volume is about tantamount to twice its radius:

$$R_c \approx 2\left(\frac{3V}{4\pi x_c N}\right)^{1/3} \tag{1}$$

The Rc was calculated around 15 using V (2255 Å^3), N (16), as well as x_c (0.08). Because of multipole–multipole interactivity, exchange interaction, or radiation reabsorption [17], [18], the non-radioactive shift between the Eu^{2+} granules are considered as the main cause for the drop of PL strength; as with x of 0.08. The power transmission of prohibited conversion and a specific space of around 5Å caused by the exchange contact [18]–[20]. According to Dexter theory, the non-radiative transitions between the Eu^{2+} ions appeared via electelecric multipolar interactions [21]–[23]. Since the 5d–4f conversion of the Eu^{2+} granule would be acceptable while the spectra PLE as well as PL are mostly separate. The following equation [24], [25] can represent I, the emitting strength for each activator dosage (x):

$$\frac{1}{x} = \frac{k}{1+\beta(x)^{\theta/3}} \tag{2}$$

where k and β indicate the continuous factors for each interaction for a given main grids; dipole–dipole, dipole–quadrupole, and quadrupole–quadrupole interactivities correspondingly have θ = 6, 8, 10. The correlation for log(I/x) with log(x) yielded a linear result. The descent (-θ/3) reached −1.92. Henceforth, θ reached around 5.76, according to the calculations. This shows that dipole–dipole controlled the Eu^{2+} emission's concentration extinguishing mechanism.

3.2. Influence of varying $Ca_2MgSi_2O_7:Eu^{2+}$ green phosphor concentration on different WLED properties

In Figure 2, a noticeable reversal in the dosages for $Ca_2MgSi_2O_7:Eu^{2+}$ (Eu-doped CAMS) and $YAG:Ce^{3+}$ is apparent. As the proportion of Eu-doped CAMS increases (ranging from 2% to 20% by weight), the dosage of $YAG:Ce^{3+}$ decreases while upholding the mean CCT levels. This adjustment maintains the medium correlated color temperature (CCT) levels and impacts the absorptivity and dispersion of light by the phosphors in WLEDs, thereby influencing the WLEDs' standard hue and luminous flux. In other words, the chromaticity and lumen output of WLED devices appears to be linked to the chosen dosage of Eu-doped CAMS. This association holds true for WLED devices operating within chromatic thermal levels spanning 6000 K to 8000 K in this paper's simulation.

The presence of Eu-doped CAMS has an effect on the transference spectrum of WLEDs as shown in Figures 3-5. The company's requirements can be used as a basis for deciding the proper phosphor amount in the WLED production. Generally, the illuminating output intensity can be slightly reduced in WLEDs that require high color accuracy. As seen in Figures 3 to 5, white illumination would be a mixture derived from the spectrum areas of 420-480 nm and 500-640 nm. The spectra in these regions rise with the concentration heightening of Eu-doped CAMS phosphor. Such an escalation in the transmission intensities can lead to the higher the lumen output intensity of the WLED, implying the capability of Eu-doped CAMS phosphor in achieving the luminous flux enhancement for high-power LED lighting applications. The data in Figure 6 can be used to validate the lumen performance of the WLED in response to the varying doped amount of Eu-doped CAMS phosphor. The outcomes in Figure 6 record that when the $Ca_2MgSi_2O_7:Eu^{2+}$ dosage ascends from 2% wt. to 20% wt., the emitted illuminating beam rises significantly. Hence, the $Ca_2MgSi_2O_7:Eu^{2+}$ is advised to used with high concentration to accomplish the notable improvement of luminosity of WLED models.

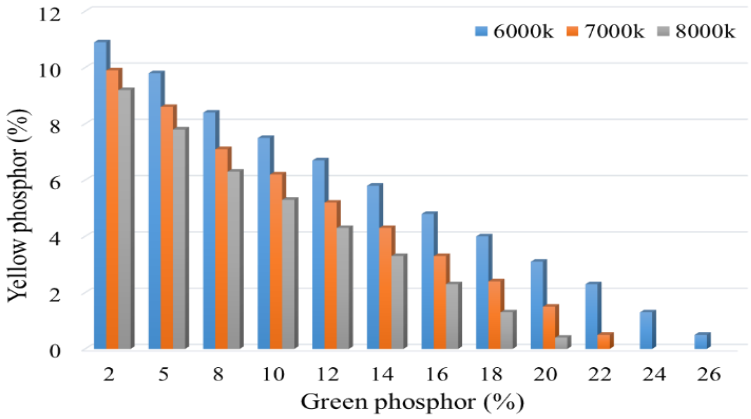

Figure 2. Shifting phosphor presence, thus sustaining median CCT

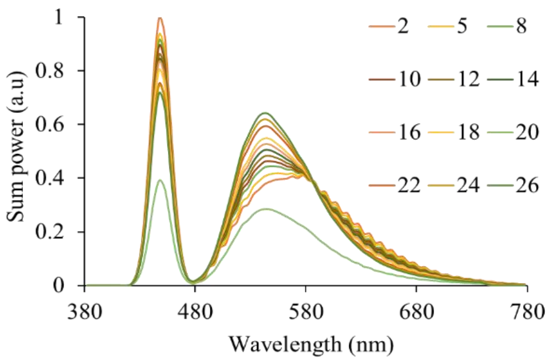

Figure 3. Relation between discharging spectra in WLED under 6000 K and $Ca_2MgSi_2O_7:Eu^{2+}$ content

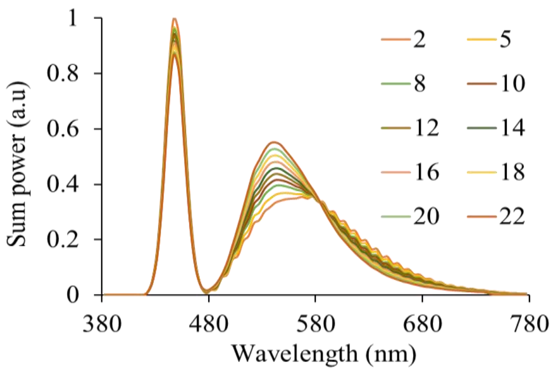

Figure 4. Relation between the emitting spectra in WLED under 7000 K and $Ca_2MgSi_2O_7:Eu^{2+}$ content

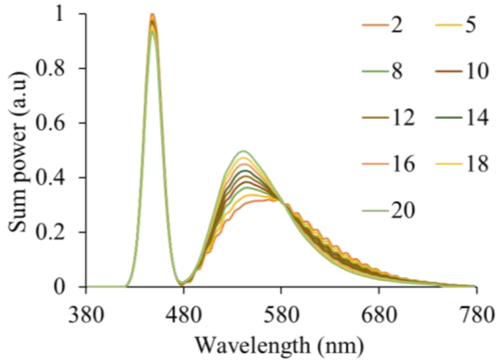

Figure 5. Relation between discharging spectra in WLED under 8000 K and $Ca_2MgSi_2O_7:Eu^{2+}$ content

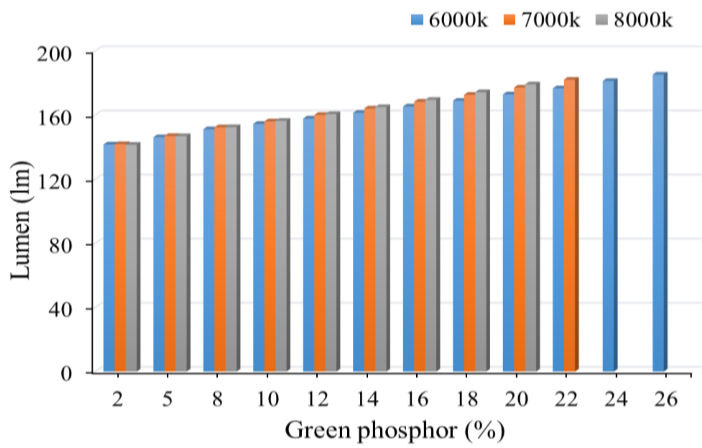

Figure 6. Relation between lumen in WLED apparatus and $Ca_2MgSi_2O_7:Eu^{2+}$ dosage

Regardless of CCT values, chromatic aberration significantly deteriorated alongside the Eu-doped CAMS content, as demonstrated by Figure 7. This also explains the absorption of the green phosphor layer. When Eu-doped CAMS absorbs the blue light emitted by the LED chip, it transforms the blue light into green light with the help of blue phosphor particles. However, the Eu-doped CAMS particles continue to absorb yellow light despite the additional blue component. Nevertheless, the material's absorption capabilities favor the absorption of blue light. Introducing Eu-doped CAMS leads to increased green component in WLEDs, which in turn improves the color consistency, a key factor in WLED lamp performance. Higher color homogeneity results in a more expensive WLED. However, the lower cost of production of the rare-erath doped silicate phosphor Eu-doped CAMS can be an advantage, making it suitable for various applications.

Chroma stability is just one of the many factors to consider when evaluating WLED chromatic performance and was not as effective as expected due to a high hue homogeneity index. Extensive studies introduced CRI and CQS. CRI determines the true chroma of objects under illumination. An imbalance in the colors blue, yellow, and green is caused by an excess of green light. This imbalance affects the hue accuracy of WLEDs. Figure 8 indicates a slight reduction in CRI with the addition of phosphor Eu-doped CAMS material. This is because CRI only demonstrates one drawback for CQS. CQS is more important and difficult to obtain than CRI, as it measures three factors: color rendering index, human preference, and chroma coordination, making it almost a universal evaluator for color performance. Furthermore, Figure 9 shows an improvement in CQS with the addition of Eu-doped CAMS phosphor when its concentration reaches 10 wt%. Beyond this concentration of Eu-doped CAMS, the CQS gradually declines, regardless of the CCT levels. This decrease is also the case with the CRI values. This can be attributed to the significant color degradation with the prevalence of green. Therefore, to achieve the desired color rendering performance, CCT uniformity, and luminous power for the WLED, choosing the right Eu-doped CAMS phosphor dosage is essential.

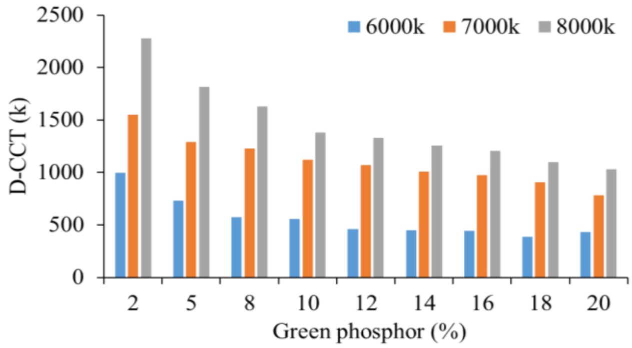

Figure 7. Relation between chroma deviation in WLED apparatus and $Ca_2MgSi_2O_7:Eu^{2+}$ dosage

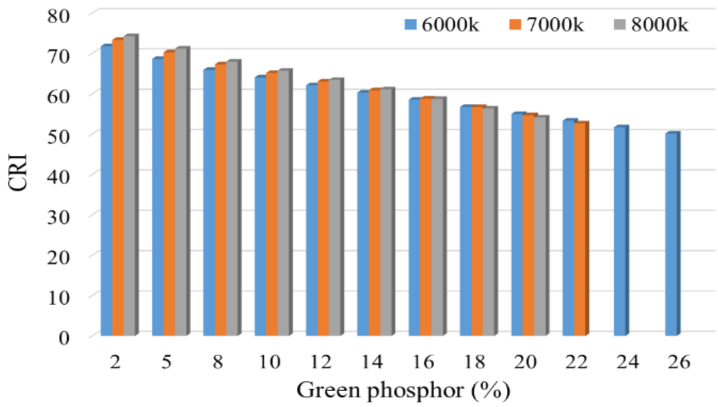

Figure 8. Relation between CRI in WLED apparatus and $Ca_2MgSi_2O_7:Eu^{2+}$ dosage

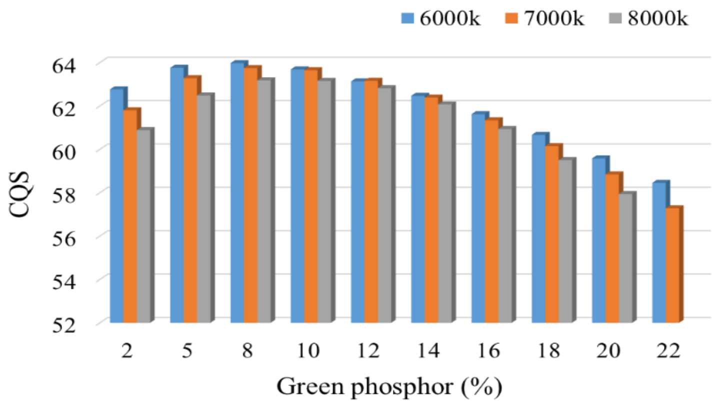

Figure 9. Relation between CQS in WLED apparatus and $Ca_2MgSi_2O_7:Eu^{2+}$ dosage

4. CONCLUSION

The paper aims to achieve the comprehensive improvements in WLED devices, using the $Ca_2MgSi_2O_7:Eu^{2+}$ green phosphor with varying concentration. Based on the obtained results, $Ca_2MgSi_2O_7:Eu^{2+}$ could enhance chroma uniformity, which works for WLED apparatuses under color heat level below 6000 K and those under color temperature exceeding 8000 K. The study herein manages to enhance chroma performance as well as the illuminating beam, by increasing the $Ca_2MgSi_2O_7:Eu^{2+}$ green phosphor concentration. Regardless, CRI, as well as CQS, have one negligible limitation. They deteriorate substantially if the $Ca_2MgSi_2O_7:Eu^{2+}$ dosage climbs excessively. As a consequence, according to the company’s objectives, the appropriate dosage must be selected. The paper offers essential information regarding creating greater chroma consistency as well as lumen for WLED apparatuses.

FUNDING INFORMATION

Authors state no funding involved.

AUTHOR CONTRIBUTIONS STATEMENT

Name of Author	C	M	So	Va	Fo	I	R	D	O	E	Vi	Su	P	Fu
Pham Van De		✓	✓	✓	✓	✓			✓	✓				
My Hanh Nguyen Thi	✓	✓	✓	✓	✓	✓	✓	✓	✓	✓	✓	✓	✓	

C : **C**onceptualization
M : **M**ethodology
So : **So**ftware
Va : **Va**lidation
Fo : **Fo**rmal analysis
I : **I**nvestigation
R : **R**esources
D : **D**ata Curation
O : Writing - **O**riginal Draft
E : Writing - Review & **E**diting
Vi : **Vi**sualization
Su : **Su**pervision
P : **P**roject administration
Fu : **Fu**nding acquisition

CONFLICT OF INTEREST STATEMENT

Authors state no conflict of interest.

DATA AVAILABILITY

The data that supports the findings of this study are openly available in:

- Materials Science- Poland [21] at https://doi.org/10.2478/msp-2020-0069.
- Reference [23] at https://doi.org/10.2478/msp-2020-007
- In OAM-RC at https://oam-rc.inoe.ro/articles/enhancing-optical-performance-of-dual-layer-remote-phosphor-structures-with-the-application-of-laaso4eu3-and-y2o3ho3/fulltext.
- Reference [24] in Telkomnika at http://doi.org/10.12928/telkomnika.v19i2.16357.
- Reference number [25] at http://doi.org/10.12928/telkomnika.v19i3.15832.

REFERENCES

[1] J. Zhou and K. Qian, "Low-voltage wide-field-of-view lidar scanning system based on a MEMS mirror," *Applied Optics*, vol. 58, no. 5, p. A283, Feb. 2019, doi: 10.1364/ao.58.00a283.

[2] C. Huang, Y. Chang, L. Han, F. Chen, S. Li, and J. Hong, "Bandwidth correction of spectral measurement based on Levenberg–Marquardt algorithm with improved Tikhonov regularization," *Applied Optics*, vol. 58, no. 9, p. 2166, Mar. 2019, doi: 10.1364/ao.58.002166.

[3] Z. Li, J. Zheng, J. Li, W. Zhan, and Y. Tang, "Efficiency enhancement of quantum dot–phosphor hybrid white-light-emitting diodes using a centrifugation-based quasi-horizontal separation structure," *Optics Express*, vol. 28, no. 9, p. 13279, Apr. 2020, doi: 10.1364/oe.392900.

[4] Y.-P. Chang *et al.*, "New scheme of LiDAR-embedded smart laser headlight for autonomous vehicles," *Optics Express*, vol. 27, no. 20, p. A1481, Sep. 2019, doi: 10.1364/oe.27.0a1481.

[5] K. Orzechowski, M. M. Sala-Tefelska, M. W. Sierakowski, T. R. Woliński, O. Strzeżysz, and P. Kula, "Optical properties of cubic blue phase liquid crystal in photonic microstructures," *Optics Express*, vol. 27, no. 10, p. 14270, May 2019, doi: 10.1364/oe.27.014270.

[6] L. Reddy, "A review of the efficiency of white light (or other) emissions in singly and co-doped dy3+ ions in different host (phosphate, silicate, aluminate) materials," *Journal of Fluorescence*, vol. 33, no. 6, pp. 2181–2192, Nov. 2023, doi: 10.1007/s10895-023-03250-y.

[7] I. Gupta, S. Singh, S. Bhagwan, and D. Singh, "Rare earth (RE) doped phosphors and their emerging applications: A review," *Ceramics International*, vol. 47, no. 14, pp. 19282–19303, Jul. 2021, doi: 10.1016/j.ceramint.2021.03.308.

[8] M. Zhao, Q. Zhang, and Z. Xia, "Structural engineering of Eu2+-doped silicates phosphors for LED applications," *Accounts of Materials Research*, vol. 1, no. 2, pp. 137–145, Nov. 2020, doi: 10.1021/accountsmr.0c00014.

[9] I. P. Sahu, D. P. Bisen, and N. Brahme, "Structural characterization and optical properties of Ca2MgSi2O7:Eu2+,Dy3+ phosphor by solid-state reaction method," *Luminescence*, vol. 30, no. 5, pp. 526–532, Aug. 2015, doi: 10.1002/bio.2771.

[10] A. Antuzevics *et al.*, "Shortwave ultraviolet persistent luminescence of Sr2MgSi2O7: Pr3+," *Materials*, vol. 16, no. 5, p. 1776, Feb. 2023, doi: 10.3390/ma16051776.

[11] H. W. Tseng, H. Y. Tu, Q. H. Yang, and C. F. Yang, "Effects of composition variations on the crystalline phases and photoluminescence properties of Ca2+ xMgSi2Eu0.025O7+ xPhosphors," *ACS Omega*, vol. 7, no. 5, pp. 3917–3924, Feb. 2022, doi: 10.1021/acsomega.1c04480.

[12] A. Adnan, Y. Liu, C.-W. Chow, and C.-H. Yeh, "Demonstration of non-hermitian symmetry (NHS) serial-complex-valued orthogonal frequency division multiplexing (SCV-OFDM) for white-light visible light communication (VLC)," *OSA Continuum*, vol. 3, no. 5, p. 1163, May 2020, doi: 10.1364/osac.391483.

[13] J. O. Kim, H. S. Jo, and U. C. Ryu, "Improving CRI and scotopic-to-photopic ratio simultaneously by spectral combinations of cct-tunable led lighting composed of multi-chip leds," *Current Optics and Photonics*, vol. 4, no. 3, pp. 247–252, 2020, doi: 10.3807/COPP.2020.4.3.247.

[14] S. Bindai, K. Annapurna, and A. Tarafder, “Realization of phosphor-in-glass thin film on soda-lime silicate glass with low sintering temperature for high color rendering white LEDs,” *Applied Optics*, vol. 58, no. 9, p. 2372, Mar. 2019, doi: 10.1364/ao.58.002372.

[15] N. A. Mica *et al.*, “Triple-cation perovskite solar cells for visible light communications,” *Photonics Research*, vol. 8, no. 8, p. A16, Aug. 2020, doi: 10.1364/prj.393647.

[16] M. Abd Elkarim, M. M. Elsherbini, H. M. AbdelKader, and M. H. Aly, “Exploring the effect of LED nonlinearity on the performance of layered ACO-OFDM,” *Applied Optics*, vol. 59, no. 24, p. 7343, Aug. 2020, doi: 10.1364/ao.397559.

[17] F. Brusola, I. Tortajada, I. Lengua, B. Jordá, and G. Peris-Fajarnés, “Parametric effects by using the strip-pair comparison method around red CIE color center,” *Optics Express*, vol. 28, no. 14, p. 19966, Jul. 2020, doi: 10.1364/oe.395291.

[18] A. Ferrero, B. Bernad, J. Campos, N. Richard, C. Fernández-Maloigne, and M. Melgosa, “Goniochromatic assessment of gray scales for color change,” *Journal of the Optical Society of America A*, vol. 37, no. 8, p. 1266, Aug. 2020, doi: 10.1364/josaa.394170.

[19] A. Alexeev, J.-P. M. G. Linnartz, K. Arulandu, and X. Deng, “Characterization of dynamic distortion in LED light output for optical wireless communications,” *Photonics Research*, vol. 9, no. 6, p. 916, Jun. 2021, doi: 10.1364/PRJ.416269.

[20] R. Fan, S. Fang, C. Liang, Z. Liang, and H. Zhong, “Controllable one-step doping synthesis for the white-light emission of cesium copper iodide perovskites,” *Photonics Research*, vol. 9, no. 5, p. 694, May 2021, doi: 10.1364/prj.415015.

[21] M. H. N. Thi, P. T. That, and N. D. Q. Anh, “Eu2+-activated strontium-barium silicate: A positive solution for improving luminous efficacy and color uniformity of white light-emitting diodes,” *Materials Science- Poland*, vol. 38, no. 4, pp. 594–600, Dec. 2020, doi: 10.2478/msp-2020-0069.

[22] N. T. P. Loan and N. D. Q. Anh, “Enhancing optical performance of dual-layer remote phosphor structures with the application of laaso4:Eu3+ and y2o3:Ho3+,” *Optoelectronics and Advanced Materials, Rapid Communications*, vol. 15, no. 1–2, pp. 71–78, 2021.

[23] P. T. That *et al.*, “Enhancing color quality of WLEDs with dual-layer remote phosphor geometry,” *Materials Science- Poland*, vol. 38, no. 4, pp. 667–674, Dec. 2020, doi: 10.2478/msp-2020-0070.

[24] H. P. Dang, P. T. That, and N. D. Q. Anh, “Utilizing CaCO3, CaF2, SiO2, and TiO2 phosphors as approaches to the improved color uniformity and lumen efficacy of WLEDs,” *Telkomnika (Telecommunication Computing Electronics and Control)*, vol. 19, no. 2, pp. 623–630, Apr. 2021, doi: 10.12928/TELKOMNIKA.v19i2.16357.

[25] M. H. N. Thi, P. T. That, and N. D. Q. Anh, “The impacts of red-emitting phosphor Mg8Ge2O11F2:Mn4+ on the color rendering index of convex-dual-layer remote phosphor WLEDs at 5600 K,” *TELKOMNIKA (Telecommunication Computing Electronics and Control)*, vol. 19, no. 3, p. 950, Jun. 2021, doi: 10.12928/telkomnika.v19i3.15832.

BIOGRAPHIES OF AUTHORS

Pham Van De received his Master's degree in Electrical Engineering from Ho Chi Minh City University of Technology and Education, Vietnam in 2015. He is currently a member of Dong Nai Technology University, Bien Hoa City, Vietnam. His research interests focus on electrical and electronic engineering and renewable energy. He can be contacted at email: phamvande@dntu.edu.vn.

My Hanh Nguyen Thi received a Bachelor of Physics from An Giang University, VietNam, Master of Theoretical Physics and Mathematical Physics, Hanoi National University of Education, VietNam. Currently, she is a lecturer at the Faculty of Mechanical Engineering, Industrial University of Ho Chi Minh City, Viet Nam. Her research interests are theoretical physics and mathematical physics. She can be contacted at email: nguyenthimyhanh@iuh.edu.vn.